DESIGN OF A QUADRUPOLE MASS SPECTROMETER FOR THE CHARACTERIZATION OF EUROPA'S ATMOSPHERE

A Project

Presented to

The Faculty of the Department of Aerospace Engineering

San José State University

In Partial Fulfillment

of the Requirements for the Degree

Master of Science

by

Jorge I. Cortés

December 2015

The Designated Project Committee Approves the Project Titled

DESIGN OF A QUADRUPOLE MASS SPECTROMETER FOR THE CHARACTERIZATON OF EUROPA'S ATMOSPHERE

By

Jorge I. Cortés

APPROVED FOR THE DEPARTMENT OF AEROSPACE ENGINEERING

SAN JOSÉ STATE UNIVERSITY

DECEMBER 2015

Dr. Nikos Mourtos	Department of Aerospace Engineering
Olenka Hubickyj 12/17/2015	
Dr. Olenka Hubickyj	Department of Physics and Astronomy

MSAE Thesis / Project Evaluation Form

Title	Design of a Quadrupole Mass Spectrometer						
Name	Jorge Cortés				Semester Fall 2015		
Advisor	Olenka Hubickyj						
Scale: 1/5 = Lacking 2/5 = Weak 3/5 = Acceptable 4/5 = Good 5/5 = Excellent							
Max Possible Score = 100		Max Possible	*Weight*	*Ave score*	Project Advisor	Faculty 2	Faculty 3
1	Application of mathematics appropriate for graduate level and the problem	5	*1*				5/5
2	Application of AE science (aerodynamics, propulsion, flight mechanics, stability & control, aerospace structures & materials, etc.) and/or aerospace vehicle design, appropriate for graduate level	20	*4*				18/20
3	Use of modern tools (computational or experimental)	10	*2*				5/5
4	Appropriate literature search (# and appropriateness of references cited)	10	*2*				5/5
5	Understanding of the cited literature (summary of previous work)	10	*2*				5/5
6	In-depth analysis and / or design of an AE system	20	*4*				19/20
7	Correct language and terminology	5	*1*				5/5
8	Ability to summarize (abstract) / draw conclusions	5	*1*				5/5
9	Appropriate use of graphs and tables	5	*1*				5/5
10	Clear project objectives	5	*1*				5/5
11	Appropriate modeling	5	*1*				5/5
	Total Score	100					97

Overall Score: 90 – 100 = Excellent, 80 – 89 = Good, 60 – 79 = Acceptable, 40 – 59 = Weak, 00 – 58 = Lacking

Comments: Jorge presented a very clear description of his project. I am an astrophysicist (computational / theory) and he explained the instrument & type of data well enough for me to understand the engineering / hardware aspect of the project. That's an accomplishment!

Non-Exclusive Distribution License for Submissions to the SJSU Institutional Repository

By submitting this license, you (the author(s) or copyright owner) grant to San Jose State University (SJSU) the nonexclusive right to reproduce, convert (as defined below), and/or distribute your submission (including the abstract) worldwide in print and electronic format and in any medium, including but not limited to audio or video.

You agree that SJSU may, without changing the content, convert the submission to any medium or format for the purpose of preservation.

You also agree that SJSU may keep more than one copy of this submission for purposes of security, back-up and preservation.

You represent that the submission is your original work, and that you have the right to grant the rights contained in this license. You also represent that your submission does not, to the best of your knowledge, infringe upon anyone's copyright.

If the submission contains material for which you do not hold copyright, you represent that you have obtained any necessary permission from the copyright owner to grant SJSU the rights required by this license, and that such third-party owned material is clearly identified and acknowledged within the text or content of the submission.

IF THE SUBMISSION IS BASED UPON WORK THAT HAS BEEN SPONSORED OR SUPPORTED BY AN AGENCY OR ORGANIZATION OTHER THAN SJSU, YOU REPRESENT THAT YOU HAVE FULFILLED ANY RIGHT OF REVIEW OR OTHER OBLIGATIONS REQUIRED BY SUCH CONTRACT OR AGREEMENT.

SJSU will clearly identify your name(s) as the author(s) or owner(s) of the submission, and will not make any alteration, other than as allowed by this license, to your submission.

I have read and accept all the terms of this license agreement:

Jorge Cortes	Digitally signed by Jorge Cortes DN: cn=Jorge Cortes, o, ou, email=cortes.jorge.ivan@gmail.com, c=US Date: 2015.12.17 16:00:02 -08'00'	12/17/2015
Signature		Date

Design of a Compact Quadrupole Mass Spectrometer for the Characterization of Europa's Atmosphere

Jorge I. Cortes*

A quadrupole mass spectrometer was designed with the ability to characterize the tenuous atmosphere of Jupiter's moon, Europa. As a constraint, this instrument was to fit within a 3U cubesat chassis without sacrificing measurement resolution or accuracy. Ion trajectories are studied through simulations carried out in the numerical computing programming language, MATLAB and the finite element analysis simulation software, COMSOL Multiphysics. Parameters are then implemented in a preliminary instrument design.

Nomenclature

A_v	Acceleration voltage
a	U dependent parameter of the Mathieu Equation of motion
$\vec{a}$	Acceleration vector
$\vec{B}$	Magnetic vector potential
e	Electronic charge
$\mathbf{E}$	Electric field
E_o	Position-independent factor
f	Frequency
f_d	Fringe field depth
$\vec{F}$	Force vector
L_{quad}	Quadrupole rod length
m_i	Ion mass
q	V dependent parameter of the Mathieu Equation of motion
r_e	Rod radius
r_0	Inscribed radius
r_o	Field radius
r_{src}	Source radius
r_{case}	Instrument case radius
t	Time
U	DC voltage
$\vec{v}$	Velocity vector
V	AC voltage
v_{xo}	Initial x-velocity of ion
α	Ratio of the frequency of an auxiliary field to ω_o
α'	Integration constants from the solution to the Mathieu equation
α''	Integration constants from the solution to the Mathieu equation
λ	Weighting factor for the x-direction of the electric field

*Graduate Student, Department of Aerospace Engineering, San Jose State University

σ Weighting factor for the y-direction of the electric field
γ Weighting factor for the z-direction of the electric field
Φ Electric potential
Φ_o Electric potential applied between opposite sets of electrodes
ξ Time expressed in terms of the applied field
ω Angular frequency of the applied field

Contents

I Introduction **5**

II Literature Review **6**
- A Introduction to Literature Review . . . 6
- B Europa's Atmosphere . . . 6
- C Europa's Surface Composition . . . 6
- D Mass Spectrometry . . . 7
- E Quadrupole Mass Spectrometers . . . 8

III Theory **10**

IV Simulations of Ion Trajectories **14**
- A MATLAB Simulations . . . 14
- B COMSOL Simulations . . . 17

V Instrument Design **24**
- A Parameters Using the Mathieu Stability Diagram . . . 24
- B COMSOL Simulations . . . 28
- C Preliminary Instrument Design through SolidWorks . . . 30

VI Conclusion **33**

List of Figures

1 Sample Mass Spectrum Plot . . . 8
2 Quadrupole Rod Arrangement . . . 9
3 Equipotential Lines for a Quadrupole Field . . . 11
4 Hyperbolic Cylinder Arrangement . . . 12
5 Mathieu Stability Equation . . . 13
6 Simulink Block Diagram for Mathieu Equation in x-direction . . . 14
7 Ion Oscillations Contained Within Instrument X-Z Plane . . . 15
8 Stable Ion Oscillations . . . 15
9 Ion Oscillations Not Contained Within Instrument X-Z Plane . . . 16
10 Unbounded Ion Oscillations . . . 16
11 Quadrupole Geometry in COMSOL . . . 18
12 Quadrupole Model in COMSOL . . . 19
13 Mesh for Simulations . . . 20
14 Free Triangular Mesh . . . 21
15 Ion Trajectories . . . 22
16 Close-up of Ion Trajectories . . . 23
17 Electric Potential Generated by Quadrupole . . . 23
18 Mathieu Stability Diagram with Mass Scan Line . . . 24
19 MATLAB Maethieu Stability Diagram . . . 25
20 Oxide Ions in X-Z Plane . . . 26
21 Oxide Ions in Y-Z Plane . . . 26
22 Sulfide Ions in X-Z Plane . . . 27
23 Sulfide Ions in Y-Z Plane . . . 27
24 Nitride Ions in X-Z Plane . . . 27
25 Nitride Ions in Y-Z Plane . . . 27
26 O^{2-} Ion Trajectories . . . 28
27 S^{2-} Ion Trajectories . . . 29
28 N^{3-} Ion Trajectories . . . 29
29 Isometric View of Quadrupole Instrument . . . 30
30 Front Profile of Quadrupole Instrument . . . 30
31 Side Profile of 3U Cubesat Chassis . . . 31
32 Isometric View of 3U Cubesat Chassis . . . 31
33 Isometric View of Partial Assembly . . . 32
34 Side Profile of Partial Assembly . . . 32

I. Introduction

The main motivation behind this project is the spirit of discovery. Space exploration is and will always be a domain of endless possibilities. It is with great motivation that I embark on this journey; a journey that will hopefully bring about insight towards methodologies used in discovering, exploring, and characterizing strange, yet oddly familiar worlds. The following encapsulates the project statement and approach.

Quadrupole mass spectrometers are scientific instruments used in mass spectrometry, an analytical technique that uses the mass-to-charge ratio of an ion in order to identify its abundance within a given sample. These types of instruments are used prevalently within the aerospace field where the main applications are in the study of planetary atmospheres and in monitoring the air quality during manned space missions. This project will deal with the development of an instrument design to characterize an atmosphere.

In order to gain insight towards design parameters, a study will first be conducted in modeling ion trajectories as they traverse a quadrupole mass spectrometer. Equations of motion will be derived and simulations will be conducted. Once done, the design iteration process will begin with the goal of restricting the size to a 3U cubesat module (30x10x10 cm) without affecting measurement resolution or accuracy.

II. Literature Review

A. Introduction to Literature Review

The following literature review will cover different articles concerning Europas atmosphere, its surface composition, and the use of quadrupole mass spectrometers.

B. Europa's Atmosphere

The existence of atmospheres on the Galilean satellites of Jupiter was first postulated circa 1970 by Steklov and Ioffe.[1] They developed a methodology where, considering the absence of strong gas sources, upper limits were obtained for gas densities in the predicted atmospheres of Io, Europa, and Callisto. Although fairly convincing, a better case was presented by Johnson et al. (1982) where high-energy ions and particles ejected from the Jovian magnetosphere cause a process known as radiolysis on Europa's surface. Radiolysis is a chemical process where the dissociation of molecules occurs via nuclear radiation. Given the known existence of Europa's top mantle composed of water ice, an O2 atmosphere was predicted due to the radiolytic decomposition of the icy surface through the bombardment of magnetospheric plasma.[10] During this process, the following chemical reactions occur:

$$H_2O \rightarrow H_2O^- + e^-$$

$$H_2O^- \rightarrow H + OH$$

$$H + H \rightarrow H_2$$

$$OH + OH \rightarrow H_2O_2$$

$$2H_2O_2 \rightarrow 2H_2O + O_2$$

it should be noted that the first reaction occurs due to water ice molecules being hit with high energy ions and particles. From here it is clear that radiolysis results in the production of H_2 molecules, O_2 molecules, and left over H_2O molecules. Considering the gaseous phase of these molecules and Europa's gravitational effect on them, the H_2 molecules are expected to drift away and escape relatively easily. On the other hand, the heavier O_2 and H_2O molecules would stay behind. It is thus easy to postulate the existence of a relatively rich oxygen atmosphere.

The O_2 atmosphere was later detected and confirmed through observations made by the Hubble Space Telescope. Through the emissions of atomic oxygen at 1304Å and 1356Å it was deduced that a tenuous O_2 atmosphere exists and that emissions come from electron impact dissociation of O_2 as opposed to electron excitation of atomic oxygen. Additionally, through their observations and analysis, Hall et al were able to calculate the surface pressure produced by the oxygen atmosphere; approximately 10^{-11} that of the Earth's atmosphere at sea level.[3]

C. Europa's Surface Composition

The main interest behind the exploration of Europa is the possibility of a vast liquid water ocean beneath the icy shell. This harbors much interest due to the high viability of organic life. Although data regarding the surface or crustal composition is limited, the sputtered atmospheric constituents and near-infrared reflectance spectra of surface regions give a lot to study.[4] This data was gathered through the Galileo Near Infrared Mapping Spectrometer investigation. The NIMS instrument had four main objectives when it was deployed on board the Galileo orbiter:[5]

1. Mapping the distribution of surface minerals on Io, Europa, Ganymede, and Callisto at 5-30 km spatial resolutions.

2. Identifying the phases and mixtures of surface minerals

3. Identifying any correlations between the observed mineralogical distributions with the solid-state imaging (SSI) system's observations of the geomorphology.

4. Determining the cloud morphology and structure of Jupiter's atmosphere over a wide range of phase angles.

The data collected during the orbit of the Galileo spacecraft around Jupiter indicates that there are regions on Europa's surface that demonstrate distorted H_2O vibrational overtone bands in the $1.5\mu m$ and $2.0\mu m$ region.[4] This is particularly interesting because it indicates that these regions contain a high concentration of solvated contaminants. In order to understand the significance of this, one must first understand the term 'solvated'. Based off of the definition provided by the International Union of Pure and Applied Chemistry (IUPAC), solvation is the process via which a solute and a solvent become stabilized. An example of this can be the ionic groups of an ion-exchange resin.[6] This is a very strong indicator of radiolysis occurring on Europa's surface. Although it had been stated before, the process of high-energy particles disassociating surface molecules was never proven to actually occur on Europa's surface. The data provided by the NIMS instrument proved to be invaluable in advancing theorized models of Europa's atmosphere and surface composition. Based off of analysis carried out, the data provided by the NIMS instrument can be interpreted one of two ways; either these regions are composed of hydrated salt minerals, or of sulfuric acid. Both hypotheses are highly plausible. The hydrated salt minerals point towards a liquid ocean beneath the mantle of ice. An ocean would explain the presence of minerals and salts on Europa's surface. During the formation of Europa, its core would have incorporated any material that could be found in the surroundings. From previous studies, it is known that Europa's core is mostly composed of silicates. If an ocean does indeed exist within Europa, the combination of tidal heating and surface erosion could bring silicates along with other minerals to the surface. These would then be encapsulated within the icy surface. Through the process of radiolysis, as previously described, these silicates and minerals would disassociate and create regions as found.

Morever, if upon further studies these regions prove to be composed of sulfuric acid, this would be easily explained by Io's high volcanic activity. The plumes erupting from Io's surface are mainly composed of sulfur (S) and sulfur dioxide ($S0_2$). Given the proximity between Io and Europa ($421{,}700km$), the content ejected by Io could reach Europa and interact with its surface.

D. Mass Spectrometry

Mass spectrometry is a broad subject that has been heavily developed since it was first introduced. This analytical technique may only require up to a few nanomoles of a sample in order to provide characteristic information regarding the analyte's structure and molecular weight.[8] What makes this a powerful technique is that, theoretically, each compound produces a unique mass spectrum; thus, this can be used in identifying the different compounds that make up an atmosphere. All mass spectrometers work in the following way: a sample vapor is introduced into the instrument and led into an ionization chamber. During this process, the sample vapor absorbs copious amounts of energy until decomposition occurs. The sample decomposes into uni-molecular samples with unique mass-to-charge ratios. From here, a specific type of mass analysis occurs depending on the type of mass spectrometer being used. The instrument then records the data and produces a mass spectrum similar to the one shown in Figure 1. Each peak corresponds to a specific molecular sample. The

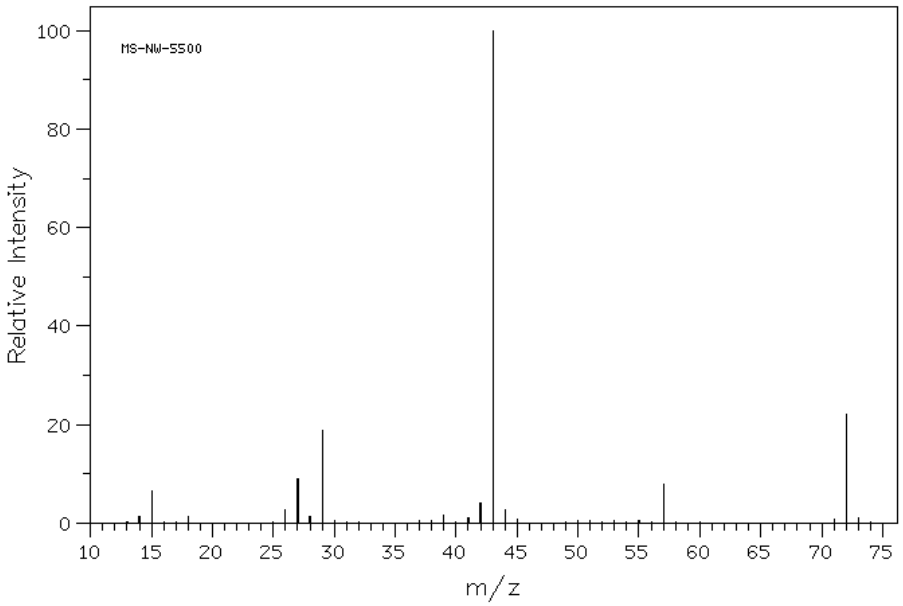

Figure 1. Sample Mass Spectrum Plot

x-axis displays mass-to-charge ratio in increasing order and the y-axis depicts a relative intensity factor in increasing order. The highest peak, known as the base peak, is used as a reference to normalize the relative abundances of all the other ions present in the disassociated sample.

E. Quadrupole Mass Spectrometers

Quadrupole mass spectrometers are a specific type of mass spectrometer that are nonmagnetic and use a combination of direct-current and radio-frequency potentials.[8] This grouping of DC and RF potentials ensures that only a predetermined molecular sample of a specific mass-to-charge ratio traverses the length of the instrument without oscillating out of control. All other samples that enter the instrument develop unbounded oscillations as they travel through the filter; this results in the ions crashing into one of the electrodes. Because these instruments are used in characterizing the composition of samples, it would be a fairly poor design if only identification of a single mass-to-charge ratio could be achieved per instrument. Thus, these instruments run sweeps of different DC and RF potentials in order to identify distinct mass-to-charge ratios. The quadrupole instrument is composed of four parallel cylindrical rods arranged in a symmetrical fashion. Opposing rods are electrically connected to RF and DC voltage generators.

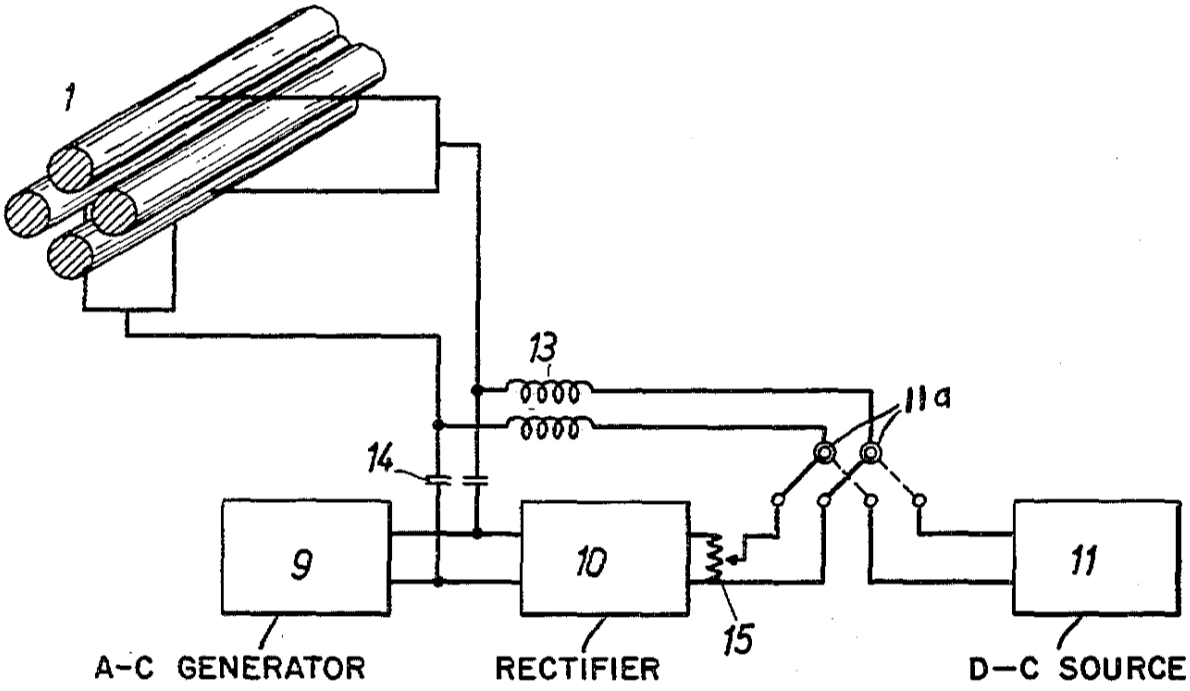

Figure 2. Quadrupole Rod Arrangement

III. Theory

The following is mostly a summary of the derivations found within Dawson's *Quadrupole Mass Spectrometry and Its Applications*. The electric field generated by the quadrupole rods is as follows:

$$\mathbf{E} = E_o(\lambda x + \sigma y + \gamma z) \tag{1}$$

It should be noted that there exists a linear dependence on the co-ordinate position. From the equation, λ, σ, and γ are weighting constants and E_o is a position-independent factor which may be a function of time.[1] Because the field is uncoupled in all three directions, the analysis of ion motion becomes quite trivial. Of course, this is assuming a perfect electric field.

Let us now consider the motion of an ion within this field. Depending on the ion's initial position, the force acting upon it varies. The further the ion is displaced from the origin, the more it experiences the effects of the force, *eE*. If we allow the field to follow restraints imposed by Laplace's equation, the following can be achieved.

$$\nabla \cdot \mathbf{E} = 0 \tag{2}$$

$$\lambda + \sigma + \gamma = 0 \tag{3}$$

If we assume $\lambda = -\sigma$ then $\gamma = 0$; likewise, if we assume $\lambda = \sigma$ then $\gamma = -2\sigma$. To better comprehend the values assumed by λ, σ, and γ, the electric potentials will be solved for. Given that $\frac{\partial \Phi}{\partial x} = E_x$, integration may be carried out that would yield Eq. (4)

$$\Phi = -\frac{1}{2}E_o(\lambda x^2 + \sigma y^2 + \gamma z^2) \tag{4}$$

If we allow $\lambda = -\sigma$ and thus $\gamma = 0$ as was previously stated, then the z term from the Eq. (4) drops out and the expression becomes as seen below.

$$\Phi = -\frac{1}{2}E_o\lambda(x^2 - y^2) \tag{5}$$

As is analogous with potential flow theory pertaining to a fluid, this represents a field composed of equipotential lines as is shown in figure X.
Four hyperbolic cylinders produce these sets of equipotential lines, where adjacent electrodes are oppositely charged. This is portrayed in figure X.
As seen above, the minimum distance between opposite electrodes is assigned the term $2r_o$. If we allow $\lambda = \frac{-1}{r_o^2}$ then the electric potential between the rods is given by the expression below.

$$\Phi = \frac{\Phi_o(x^2 - y^2)}{2r_o^2} \tag{6}$$

From here, expressions for the electric field in the x and y direction can be obtained.

$$E_x = \frac{\Phi_o x}{r_o^2} \tag{7}$$

$$E_y = \frac{-\Phi_o y}{r_o^2} \tag{8}$$

Attention is now turned towards obtaining the equations of motion. Let us start our motion analysis as with any other case; considering Newton's Law.

$$\vec{F} = m\vec{a} \tag{9}$$

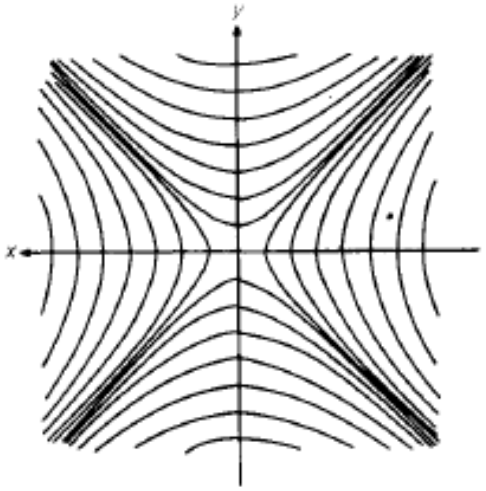

Figure 3. Equipotential Lines for a Quadrupole Field

From the Lorentz Force, we have the equation below; where e is the electric charge.

$$\vec{F} = e[\vec{E} + (\vec{v} \times \vec{B})] \tag{10}$$

This provides the force due to an electric and magnetic field. We are only concerned with the force due to an electric field since quadrupole mass spectrometers are nonmagnetic instruments; therefore, the equation below becomes the expression for force.

$$\vec{F} = e\vec{E} \tag{11}$$

We can thus rewrite Newton's Second Law as

$$e\vec{E} = m\vec{a} \tag{12}$$

Utilizing the Eq. (7) and Eq. (8), the equations of ion motion become

$$\ddot{x} + (\frac{e}{mr_o^2})\Phi_o x = 0 \tag{13}$$

$$\ddot{y} - (\frac{e}{mr_o^2})\Phi_o y = 0 \tag{14}$$

If it is assumed Φ_o is constant and the term A is defined as

$$A = (\frac{e}{mr_o^2})\Phi_o \tag{15}$$

The equations of motion may then be simplified to

$$\ddot{x} = -Ax \tag{16}$$

$$\ddot{y} = Ay \tag{17}$$

These are second-order ordinary differential equations with the following trivial solutions

$$x = c_1 \sin\sqrt{A}t + c_2 \cos\sqrt{A}t \tag{18}$$

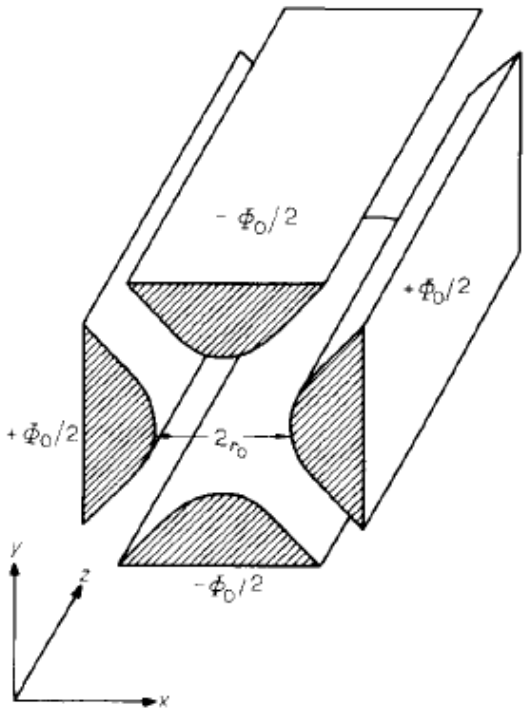

Figure 4. Hyperbolic Cylinder Arrangement

$$y = c_1 e^{\sqrt{A}t} + c_2 e^{-\sqrt{A}t} \tag{19}$$

The solution for $x(t)$ yields simple harmonic motion within the $x-z$ plane; on the other hand, $y(t)$ yields unstable motion within the $y-z$ plane. The term Φ_o is not constant however. Instead, it is (usually) a periodic function as follows

$$\Phi_o = (U - V\cos\omega t) \tag{20}$$

Therefore, the equations of motion become

$$\ddot{x} + (\frac{e}{mr_o^2})(U - V\cos\omega t)x = 0 \tag{21}$$

$$\ddot{y} - (\frac{e}{mr_o^2})(U - V\cos\omega t)y = 0 \tag{22}$$

These equations of motion take the general form of Hill's Differential Equation

$$\frac{d^2y}{dt^2} + f(t)y = 0 \tag{23}$$

where the function $f(t)$ is periodic. In order to simplify analysis, the following terms are defined

$$a_u = a_x = -a_y = \frac{4eU}{m\omega^2 r_o^2} \tag{24}$$

$$q_u = q_x = -q_y = \frac{2eV}{m\omega^2 r_o^2} \tag{25}$$

$$\xi = \frac{\omega t}{2} \tag{26}$$

This allows the equations of motion to be written in a more compact manner where u represents either x or y.

$$\frac{d^2u}{d\xi^2} + (a_u - 2q_u \cos 2\xi)u = 0 \tag{27}$$

Eq. (27) is now in the form of the Mathieu Equation in canonical form, which is a special case of Hill's Differential Equation. Solutions of the Mathieu Equation are well known and have been prevalently studied. The solution to Eq. (27) is as follows

$$u = \alpha' e^{\mu\xi} \sum_{n=-\infty}^{\infty} C_{2n} e^{2in\xi} + \alpha'' e^{-\mu\xi} \sum_{n=-\infty}^{\infty} C_{2n} e^{-2in\xi} \tag{28}$$

Stable regions for ions with specific mass-to-charge ratios can be obtained based off of the Mathieu stability diagram where a specific D.C. and R.F. voltage will yield sustained oscillations as the ion traverses the instrument.

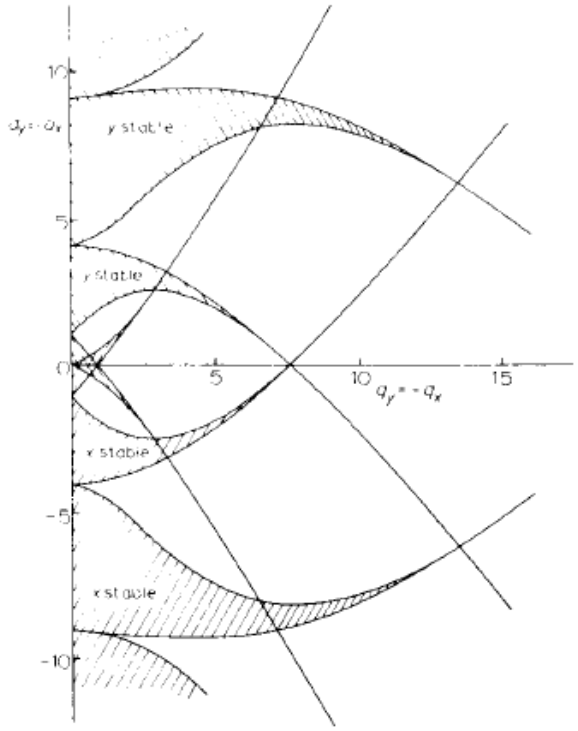

Figure 5. Mathieu Stability Equation

IV. Simulations of Ion Trajectories

A. MATLAB Simulations

As a preliminary study, the equations of motion are modeled in MATLAB's Simulink toolbox. The block diagram for the motion of an ion within the x-z plane of the instrument is seen in Figure 6. The results shown here are for an atomic mass of 16 and 32. The inscribed radius, r_o, was set at $0.005mm$ and the voltage potentials were chosen to favor the ion of 16 amu. As can be seen from Figure 7 and 8, the 16 amu ion has oscillations well within the $0.005mm$ threshold of the instrument. On the other hand, as can be seen from figures 9 and 10, the 32 amu ion also has sustained oscillations; however, these are outside the boundary set by the inscribed radius.

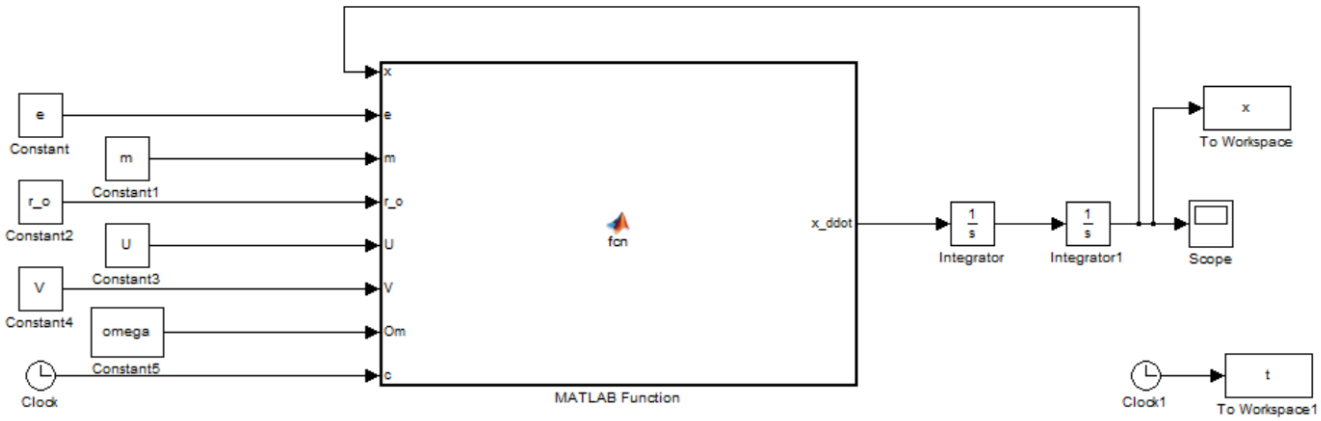

Figure 6. Simulink Block Diagram for Mathieu Equation in x-direction

The MATLAB function seen in the block diagram is found below.

```
function x_ddot = fcn(x,e,m,r_o,U,V,Om,c)
%Mathieu equation representing ion trajectory motion within the
   quadrupole

x_ddot = -(((2*e)/(m*r_o^2))*(U-V*cos(Om*c)))*x;
end
```

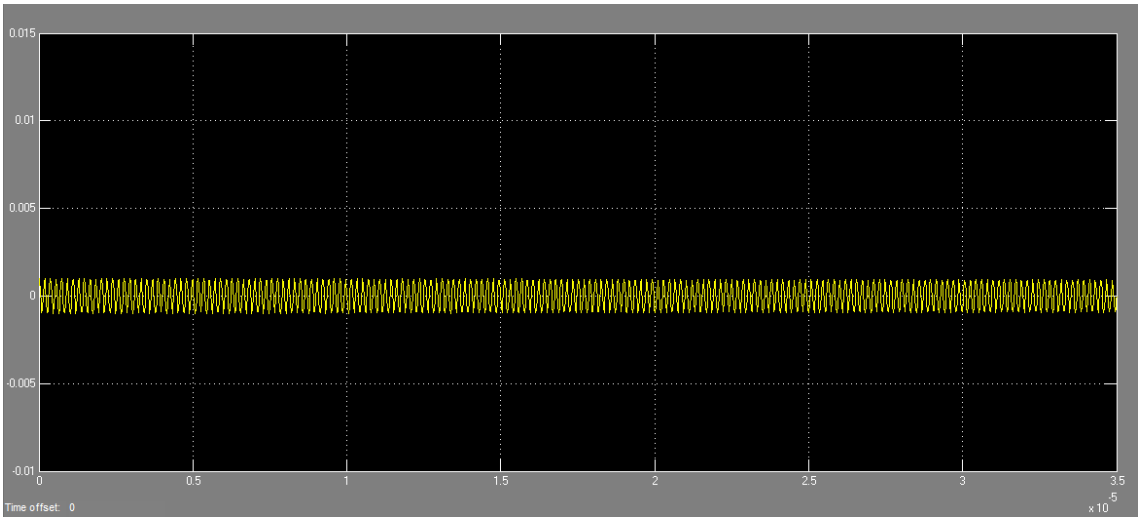

Figure 7. Ion Oscillations Contained Within Instrument X-Z Plane

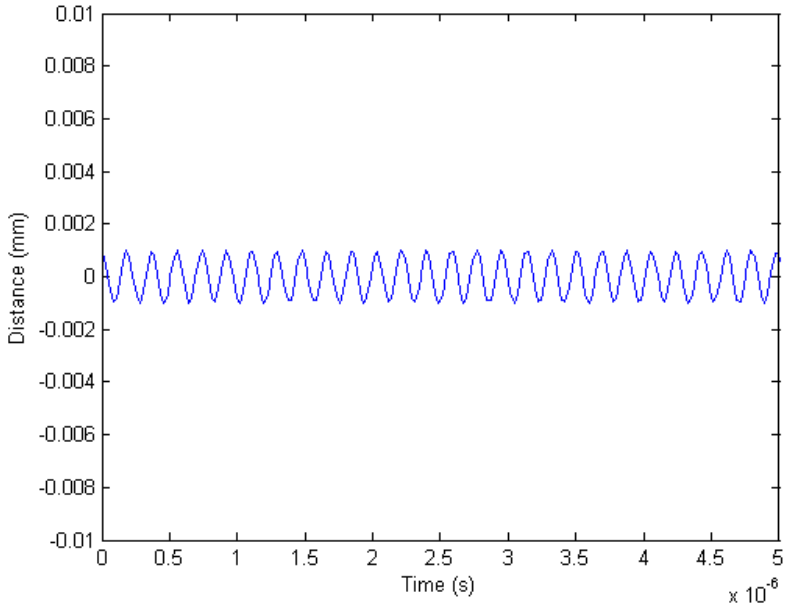

Figure 8. Stable Ion Oscillations

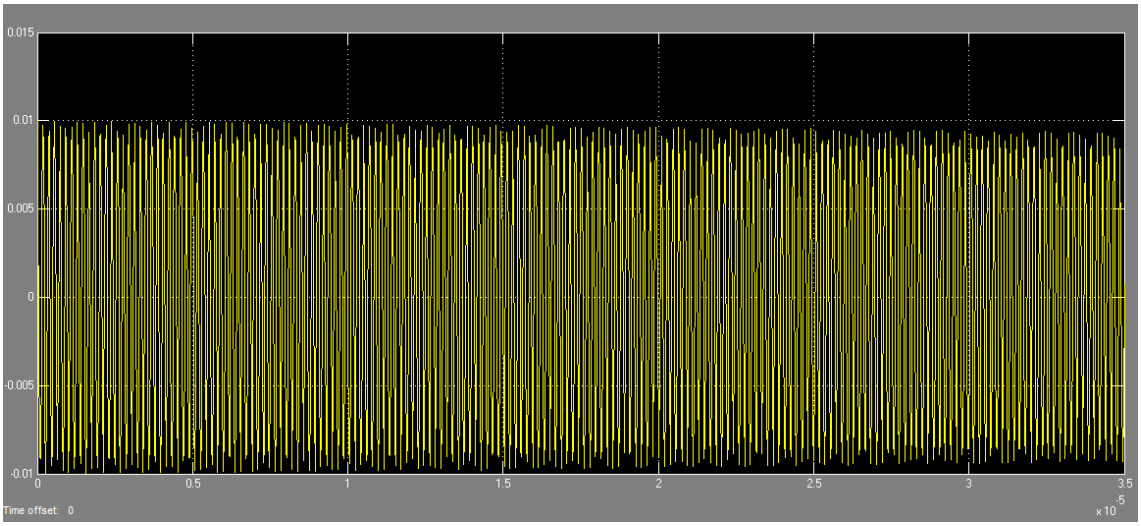

Figure 9. Ion Oscillations Not Contained Within Instrument X-Z Plane

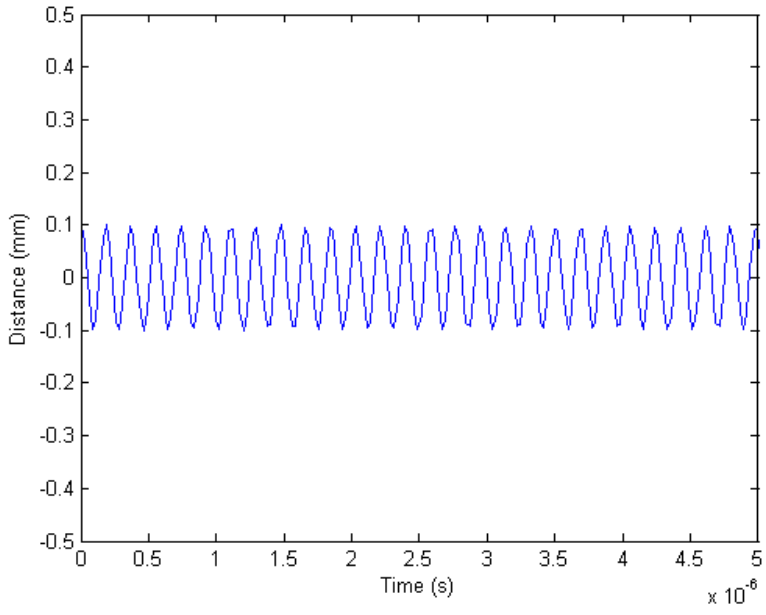

Figure 10. Unbounded Ion Oscillations

B. COMSOL Simulations

To further analyze the motions of ions, the COMSOL Multiphysics software package was used.[a] Due to their expansive library, documentation for modeling ions within a quadrupole mass spectrometer was found. The modeling process is as follows.

A 3D modeling file is initiated with the Electrostatics, Electric Currents, and Charged Particle Tracing modules added. The following quadrupole parameters are then defined. Once the parameters are saved, the quadrupole geometry is built. 4 circles with a radius of r_e are drawn within the y-z plane and are placed at a distance of $2r_e$ from the origin. The circles are then extruded out to a length of L_{quad}. A new y-z working plane is now created placed at a distance of f_d from the original one; this will be the initial position of the injected ions. 3 circles are drawn on this new plane; one with a radius of r_{case} for the enclosure of the quadrupole, another with a radius of r_{src} for the ion source, and a last one with a radius of $2r_{src}$. The last circle is created to have a tightly spaced mesh for the ion source. As before, an extrusion is made; one with a length of f_d and another with a length of L_{quad}. A difference is done between the two extrusions.

Table 1. Initial Quadrupole Parameters

Name	Expression	Value	Description
r_e	$2.768\ mm$	$2.768 \times 10^{-3}\ m$	Rod radius
r_0	$\frac{r_e}{1.147}\ mm$	$2.4133 \times 10^{-3}\ m$	Inscribed radius
r_{src}	$0.75\ mm$	$7.5 \times 10^{-4}\ m$	Source radius
r_{case}	$4r_e\ mm$	$1.1072 \times 10^{-2}\ m$	Case radius
L_{quad}	$127\ mm$	$.127\ m$	Quadrupole length
a	0.05	0.05	Mathieu coefficient
q	0.7	0.7	Mathieu coefficient
f	$4\ MHz$	$4 \times 10^6\ Hz$	Frequency
ω	$2\pi f$	$2.5133 \times 10^7\ Hz$	Angular frequency
m_i	$40\ amu$	$6.6422 \times 10^{-26}\ kg$	Ion mass
V_{ac}	$\frac{qm_i\omega^2 r_0^2}{4e}$	$266.88\ V$	AC voltage
U_{dc}	$\frac{ami\omega^2 r_0^2}{8e}$	$9.5316\ V$	DC voltage
A	$2\ V$	$2\ V$	Accelerating voltage
v_{x0}	$\sqrt{\frac{2eA}{m_i}}$	$3106.2\ m/s$	Initial x velocity
f_d	$2\ mm$	$2\ mm$	Fringe field depth

[a] A free trial was obtained through COMSOL, Inc.

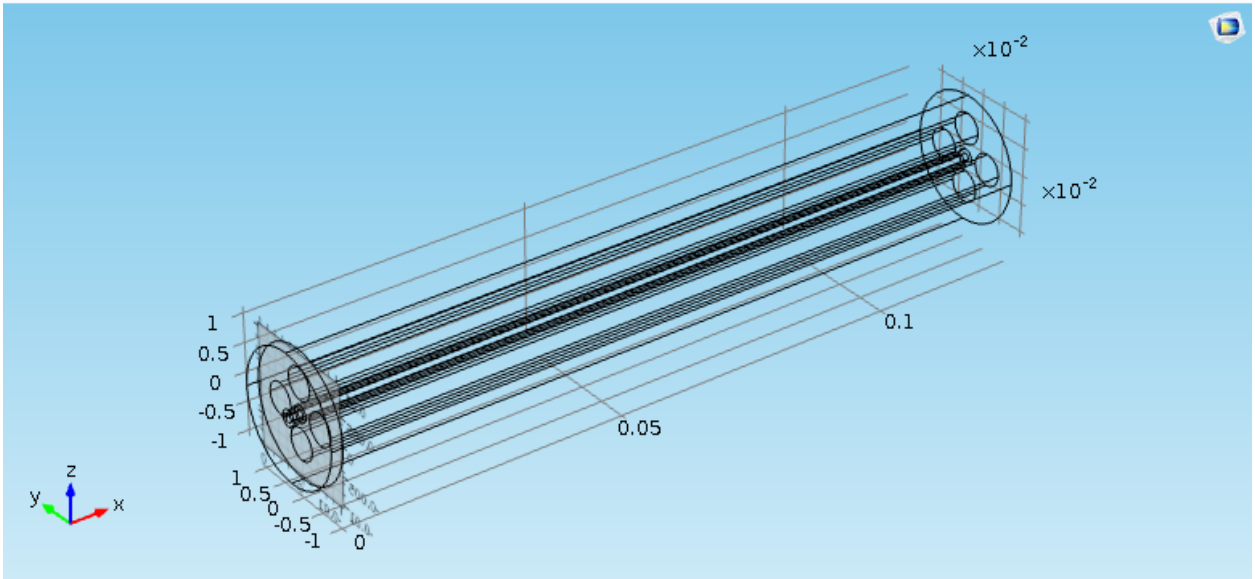

Figure 11. Quadrupole Geometry in COMSOL

The quadrupole rods are then defined as either being positively or negatively charged. To do this, a wire-frame rendering of the geometry is created. The boundaries for the positive rods are renamed *Positive* and the boundaries for the negative rods are renamed *Negative*. This is done to easily identify each one when setting the electrostatic parameters. Boundaries labeled as *Positive* are assigned an electric potential field of U_{dc} and those labeled *Negative* are assigned $-U_{dc}$. Electric currents for the rods are now defined. The *Positive* boundaries are given an electric potential field of V_{ac} and the *Negative* boundaries are given $-V_{ac}$.

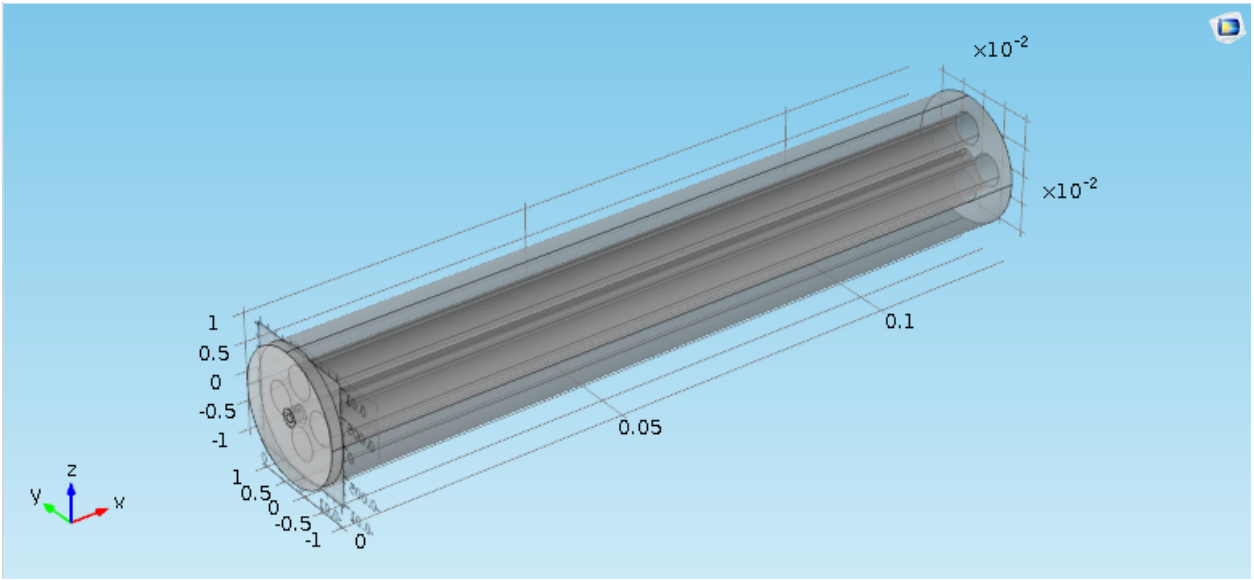

Figure 12. Quadrupole Model in COMSOL

Ion particles are defined through the *Charged Particle Tracing* node. A particle mass of m_i and a charge number of $Z = 1$ is set. 100 particles are released per release, with 11 releases in total per simulation. Ion injections occur within a time range of $2.5 \times 10^{-7} s$; with releases occurring at equal time partitions. All particles have an initial x-velocity as defined in Table 1. There are no velocity components in the y or z direction.

The material for the rods and distinct parts of the spectrometer are left unspecified. The only material characteristics set are relative permittivity (ε_r) and electrical conductivity (σ). Since this instrument is to be utilized in space, ε_r is set to 1 since it is defined this way for a vacuum. Electrical conductivity is set to 0

To conduct simulations, meshing must be done. An extra-fine triangular mesh is done at the front and back face of the instrument. As seen from the figure, the spacing gradually changes as the radius increases. A tighter mesh spacing is of interest towards the center in order to provide higher fidelity calculations for the injected ions. The rest of the geometry is given a rectangular mesh with the default spacing. Because we are primarily interested with the ion motion, meshing efforts are focused for the area of the injected ions and the rest of the instrument can be given a default mesh spacing.

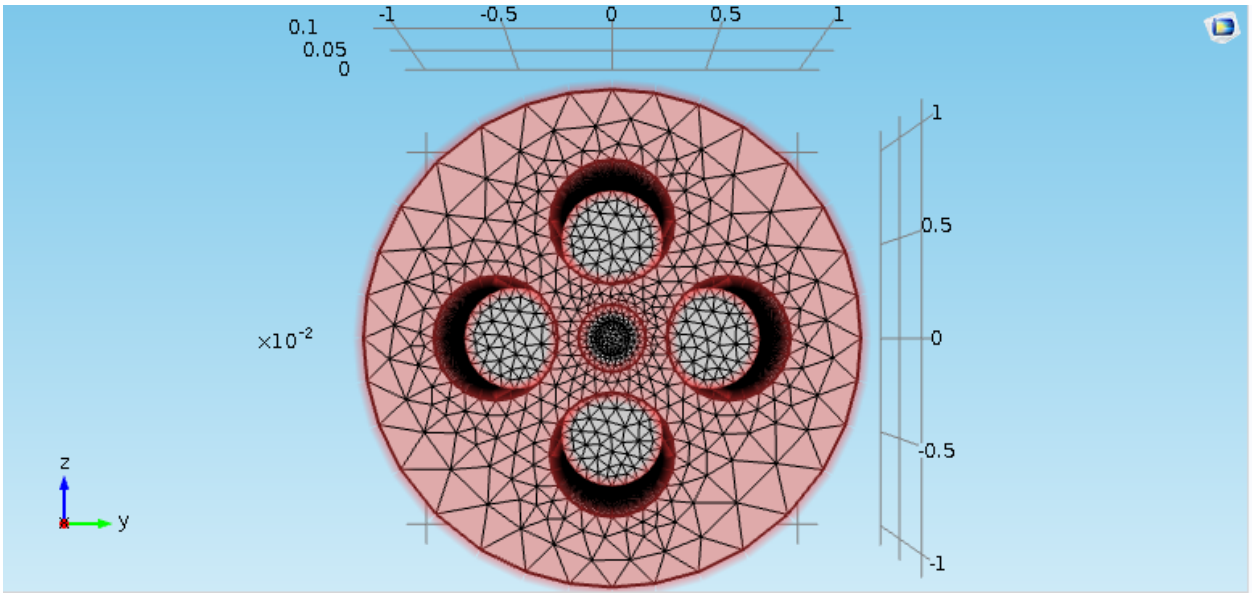

Figure 13. Mesh for Simulations

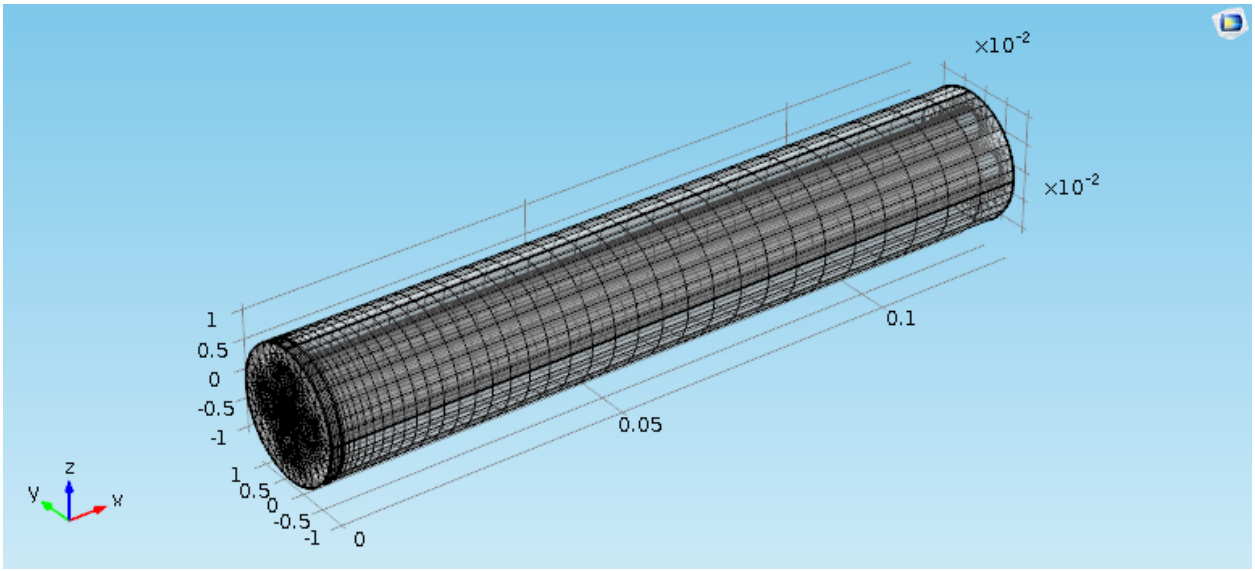

Figure 14. Free Triangular Mesh

Prior to running simulations, appropriate studies must be added to the model. For this particular case, 3 studies are conducted: an electrostatic study, an electric currents study, and a particle tracing study. After conducting simulations, results demonstrate the ions traversing the instrument with sustained oscillations as can be seen in the figures below. Although not demonstrated, all other particles with a distinct mass-to-charge ratio would not make it to the end of the instrument; instead, the ions would be absorbed by the rods. As a sanity check, the electric potential profile is calculated and is depicted below. The voltage varies between -8 and 8 as expected and the profile is reminiscent of equipotential lines; depicted in Figure 17.

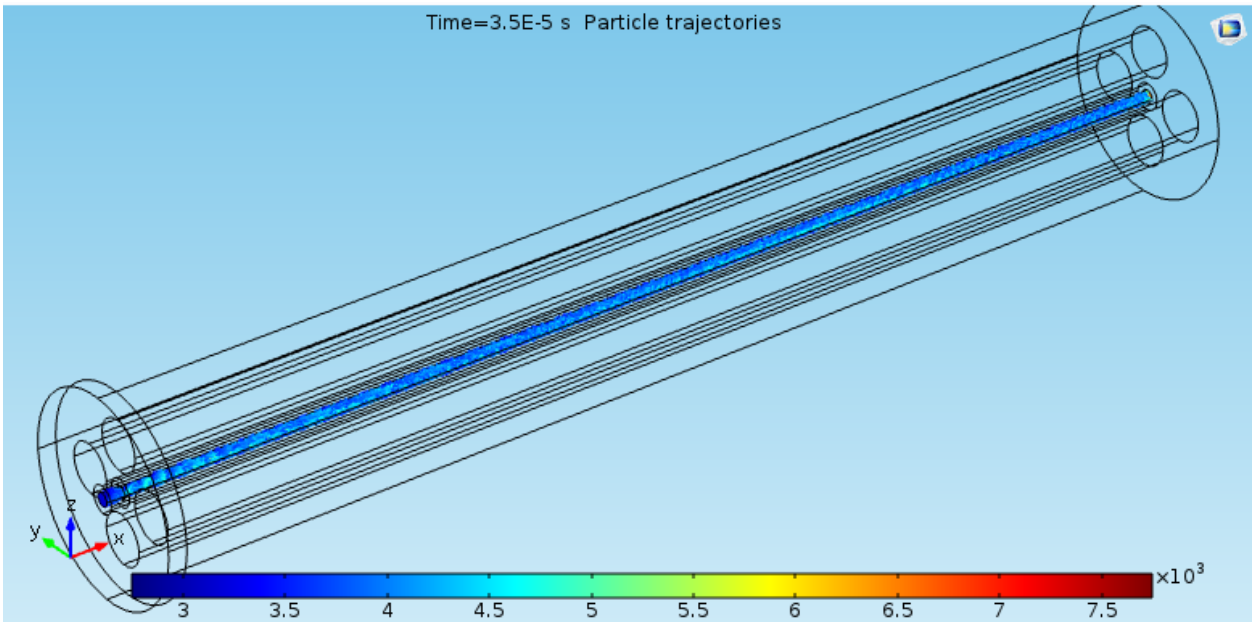

Figure 15. Ion Trajectories

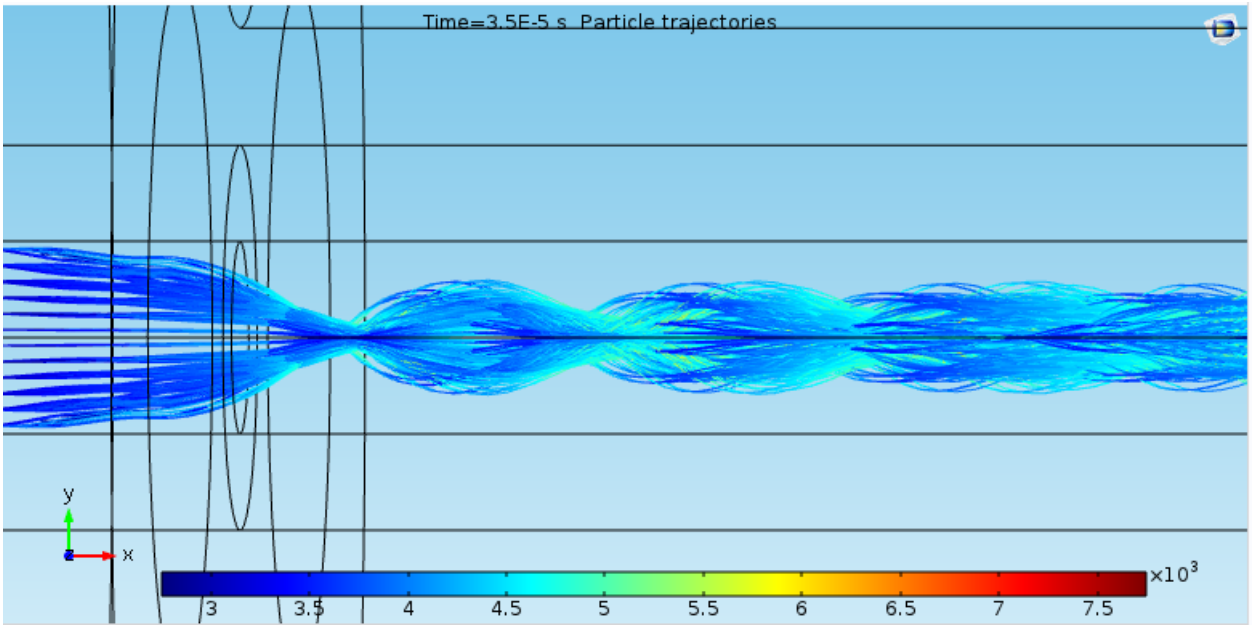

Figure 16. Close-up of Ion Trajectories

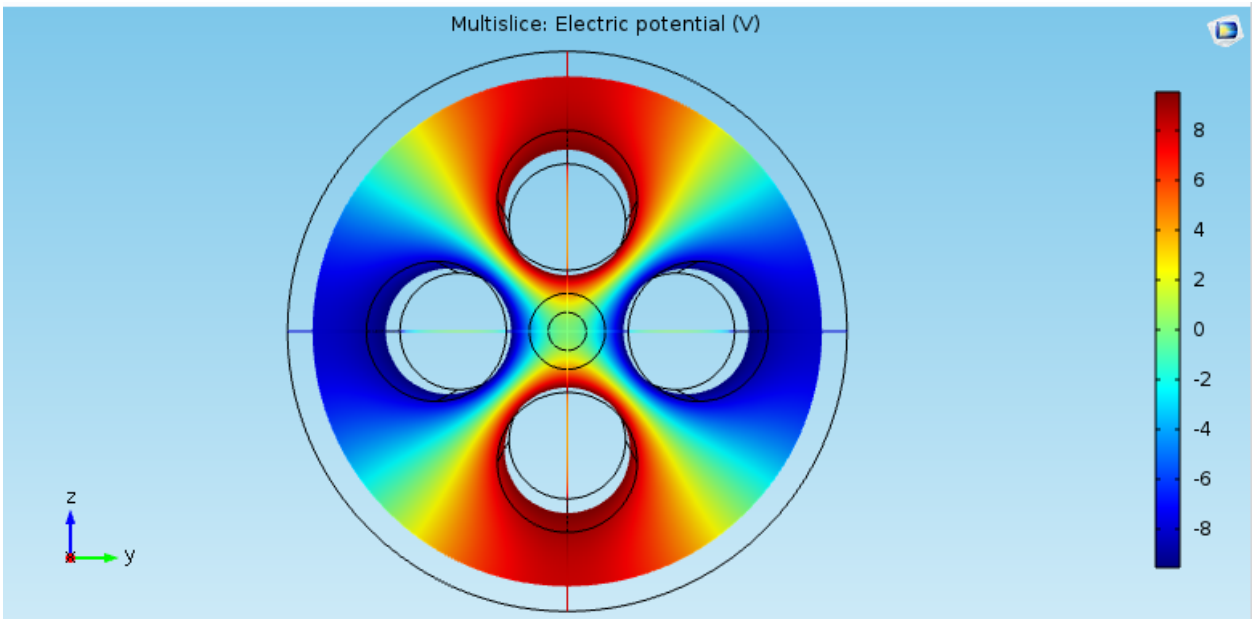

Figure 17. Electric Potential Generated by Quadrupole

V. Instrument Design

A. Parameters Using the Mathieu Stability Diagram

A preliminary design is conducted using the parameters from the COMSOL simulations. Given that a goal of this project is to fit the instrument within a 3U cubesat, using the simulation geometry is advantageous due to its already compact size. Recalling from Eq. (24) and Eq. (25), our main design variables are U, ω, r_o, and V. Since the operational frequency and the inscribed radius are already set, this only leaves the AC voltage and the DC voltage as tunable parameters. As stated within the literature review, the main interest in studying Europa's atmosphere is due to the possible oxygen present from the radiation bombardment of its icy shell. Since oxygen is of main interest, the instrument is designed with this as the base point. Having a selectivity towards O_2 will allow us to characterize the abundance within the atmosphere.

As can be seen in the figure below, the ratio of a to q, which are the coefficients of the Mathieu Equation, yield a mass scan line that crosses a section of the stability diagram. Depending on the ratio, the mass scan line can cover a narrow area of the diagram. This case corresponds to the equivalent of a narrow bandpass filter. Appropriately tuning the ratio between a and q will result in stable motion for a single mass-to-charge ratio. Or a small range of mass-to-charge ratios.

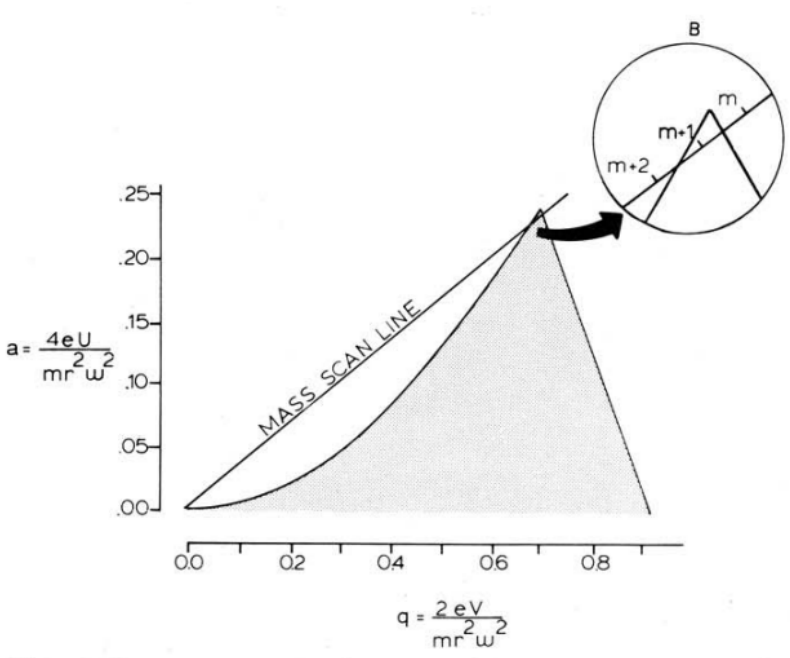

Figure 18. Mathieu Stability Diagram with Mass Scan Line

Slightly modifying a code developed by Dr. Siva Srinivas Kolukula of the Gandhi Centre for Atomic Research (IGCAR),[12] a MATLAB plot for the Mathieu stability diagram is obtained. Considering that it is of main interest to classify the oxygen abundance within Europa's atmosphere, a mass scan line of steep slope can be used to increase the instrument's sensitivity towards a specific ion. A mass scan line of $a/q = 0.3$ is chosen and is depicted in Figure 19.

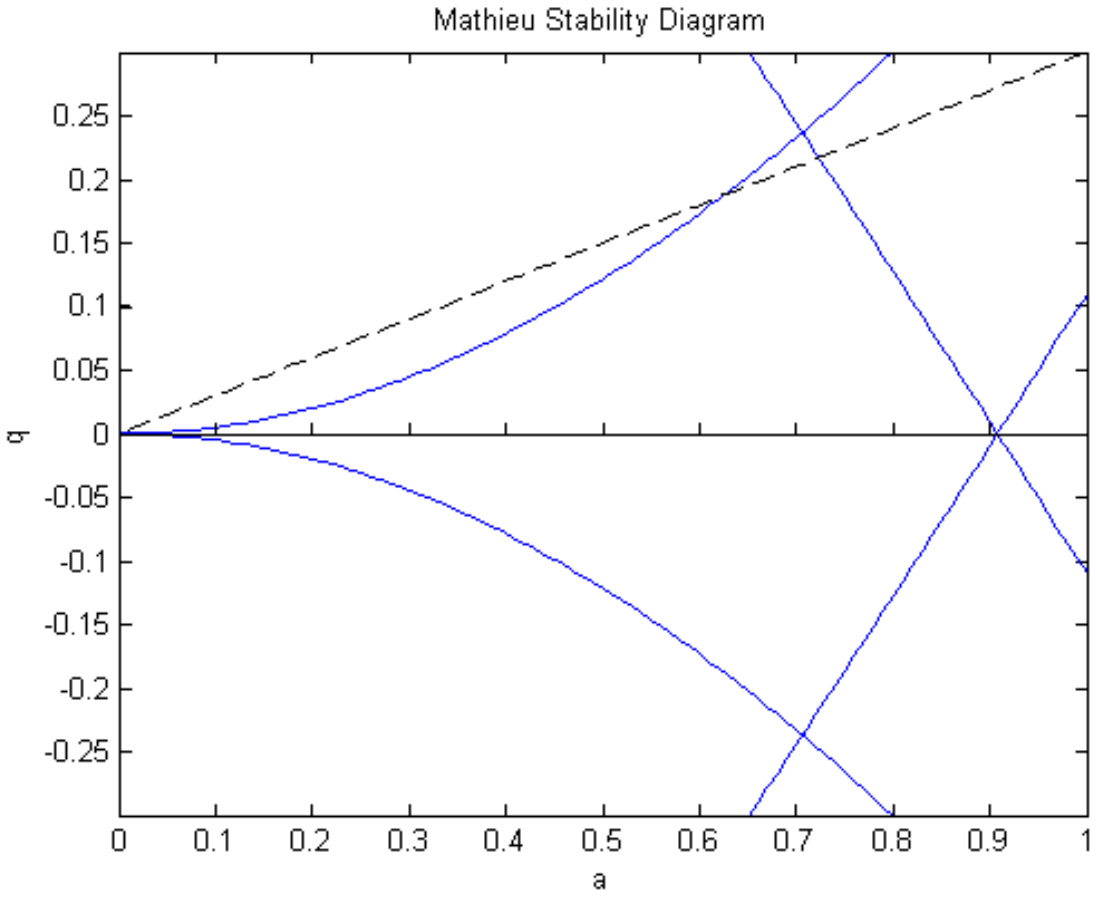

Figure 19. MATLAB Maethieu Stability Diagram

In order to keep operating voltages at a minimum, the instrument is chosen to function within the first stability region. This restricts the values of a and q to fall within 0 - 0.9 and 0 - 0.23, respectively. After several iterations in MATLAB, $a = 0.21$ and $q = 0.7$ are settled upon as these values result in the oxide ion having sustained oscillations within the X-Z and Y-Z plane of the instrument. From the preliminary COMSOL simulations, the initial x-velocity is defined as $\sqrt{\frac{2eA}{m_i}}$. A very important distinctions must be made: The preliminary COMSOL simulations were done with the x-axis aligned with the direction of travel for the ions. This is not the case for the MATLAB and further COMSOL simulations. Instead, the z-axis is aligned with the direction of travel.

In conducting the simulations, the voltages were chosen to favor the O^{2-} ion. When other samples were simulated, these voltages remained constant and where used to calculate new values for a and q pertaining to that sample, as shown below:

$$a = \frac{8eU_{dc}}{m\omega^2 r_0^2}$$

$$q = \frac{4eV_{ac}}{m\omega^2 r_0^2}$$

Additionally, the travel time of the ion is calculated by simply dividing the length of the instrument by the initial z-velocity. This will provide a good approximation to the estimated Δt. Figure 20 through Figure 25 depict the results for O^{2-}, S^{2-}, and N^{3-}. The maximum values for the y-axes are set to the instrument radius to easily identify whether the ion motions are bounded within the instrument. As can be seen, the motion in the X-Z and Y-Z plane for O^{2-} remains within the instrument and is able to traverse the instrument. This, however, is not the case for the other ions. The S^{2-} ion has sustained oscillations within the X-Z plane but the motion within the Y-Z plane is unstable. This leads to the net result of the ion crashing into the rods. A similar situation is seen with the N^{3-} ion. Stable motion is seen in the Y-Z plane but is unstable within the X-Z plane. As expected, only the O^{2-} ions are able to go through the instrument.

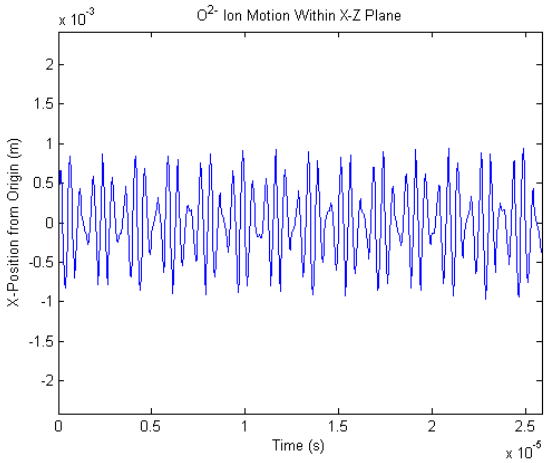

Figure 20. Oxide Ions in X-Z Plane

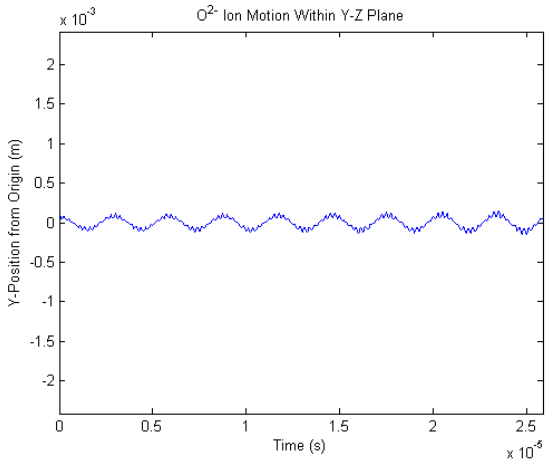

Figure 21. Oxide Ions in Y-Z Plane

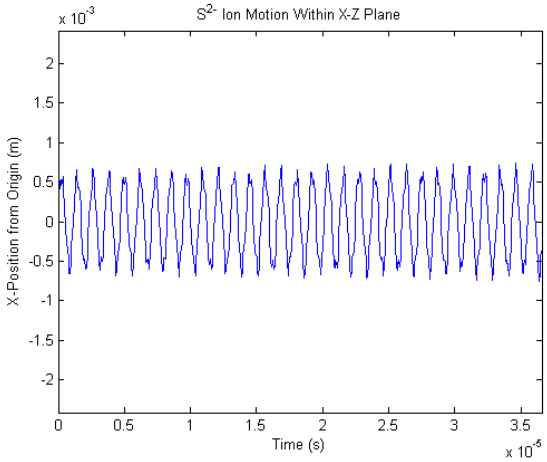

Figure 22. Sulfide Ions in X-Z Plane

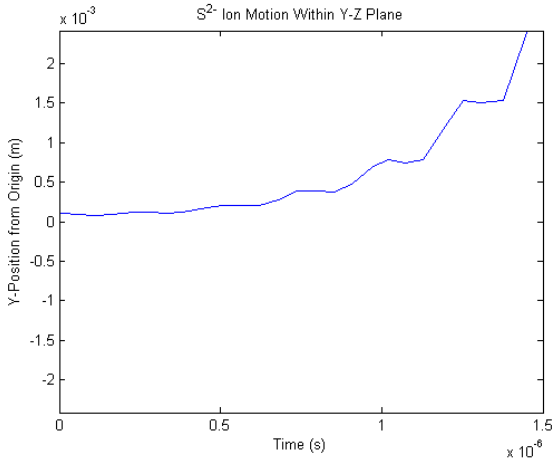

Figure 23. Sulfide Ions in Y-Z Plane

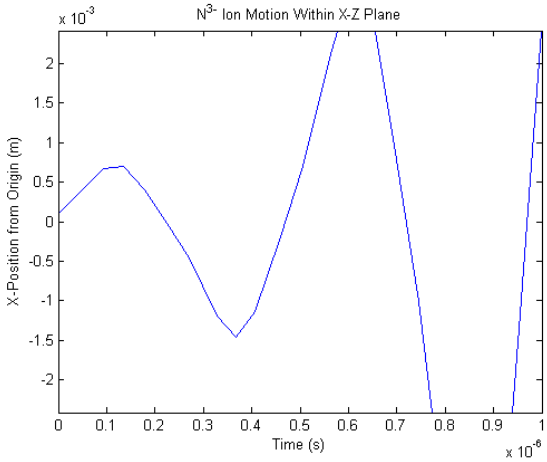

Figure 24. Nitride Ions in X-Z Plane

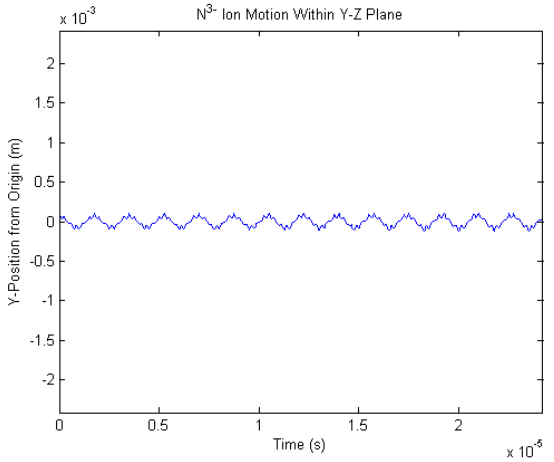

Figure 25. Nitride Ions in Y-Z Plane

B. COMSOL Simulations

The acquired a and q values will be implemented via a script that will control the voltage generators. Although this project does not deal with the design of the necessary circuits or power system, an iteration is done through COMSOL to simulate the ion trajectories with the chosen values for a and q. Table 2 summarizes the parameters used. The instrument geometry remains unchanged and is described by Table 1.

Table 2. Quadrupole Parameters

Name	Expression	Value	Description
a	0.21	0.21	Mathieu coefficient
q	0.7	0.7	Mathieu coefficient
m_o	16 amu	2.6569×10^{-26} kg	Oxide Ion mass
m_s	32 amu	5.3137×10^{-26} kg	Sulfide Ion mass
m_N	14 amu	2.3248×10^{-26} kg	Nitride Ion mass
V_{ac}	$\frac{qm_o\omega^2 r_0^2}{4e}$	106.9 V	AC voltage
U_{dc}	$\frac{am_o\omega^2 r_0^2}{8e}$	16.04 V	DC voltage

Utilizing the same procedure as previously described, simulations for the O^{2-} ions result in bounded oscillations. As can be seen from Figure 26, the ions successfully traverse the instrument.

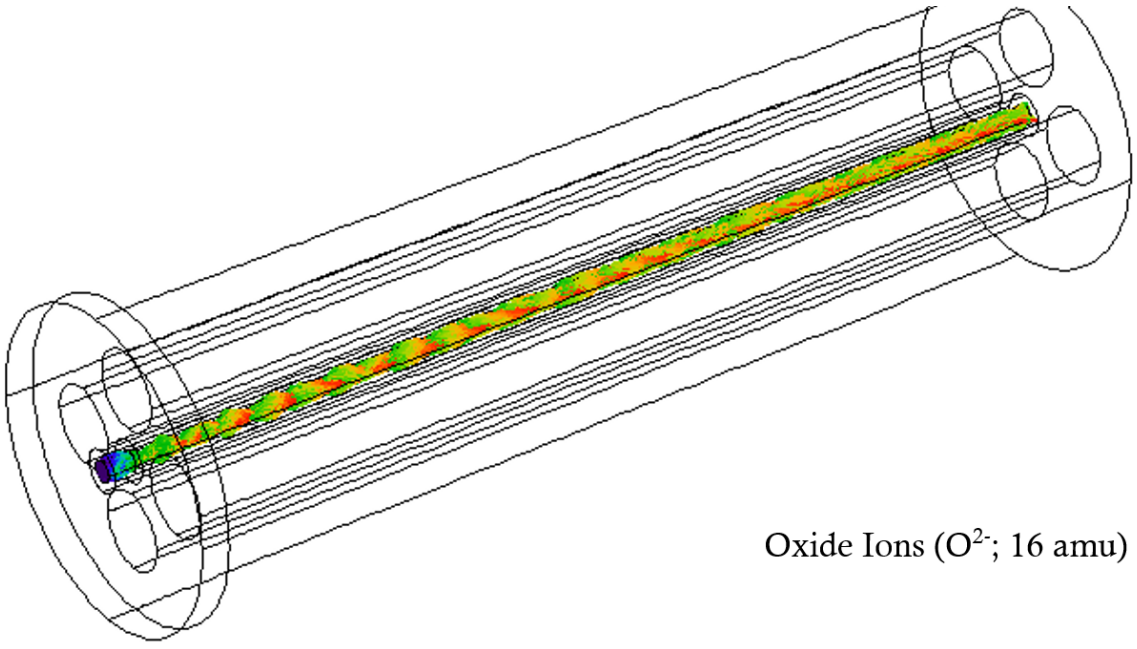

Figure 26. O^{2-} Ion Trajectories

Considering now the behavior of the S^{2-} and N^{3-}, we see from Figure 27 and Figure 28 that the ions crash into the rods; in fact, it is noticed that the behavior of both ions are reminiscent of the behavior seen from the unstable motions produced from the MATLAB simulations.

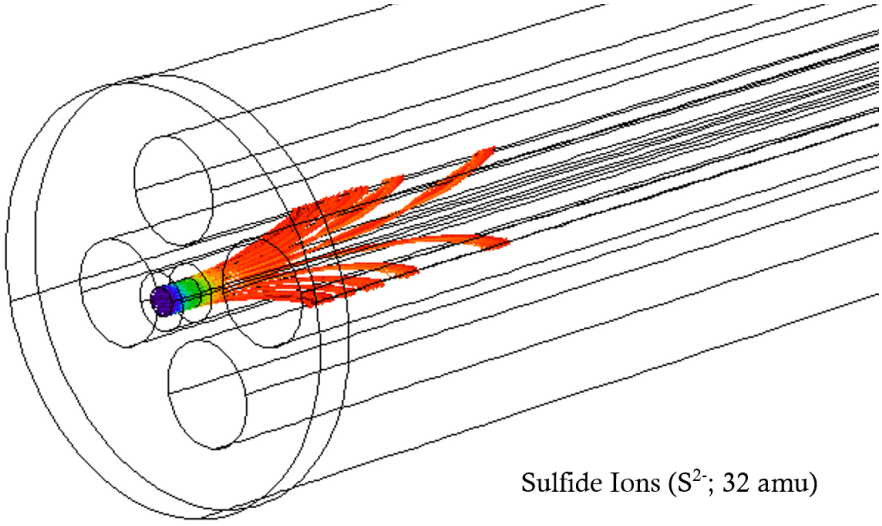

Figure 27. S^{2-} **Ion Trajectories**

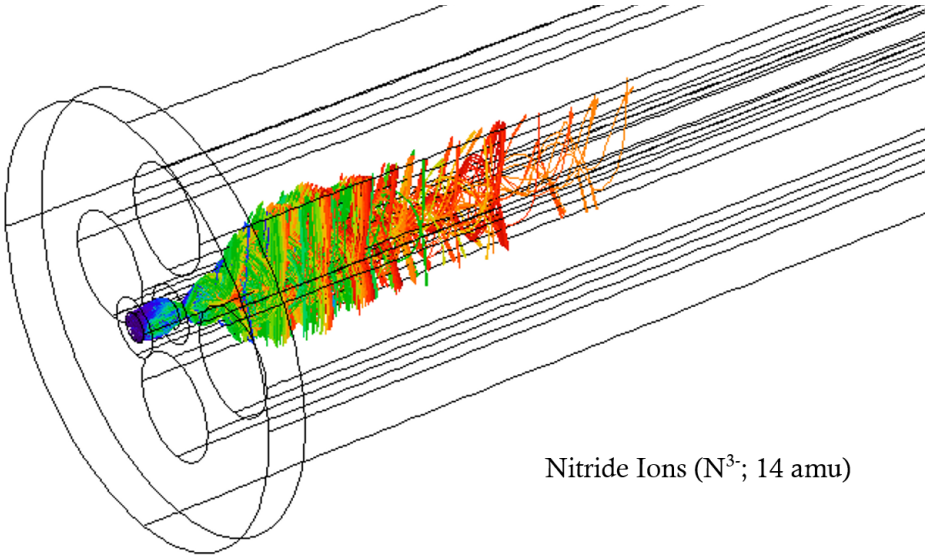

Figure 28. N^{3-} **Ion Trajectories**

C. Preliminary Instrument Design through SolidWorks

The CAD/CAE software program, SoldWorks, is used in creating a model of the instrument design that utilized the parameters tested through the MATLAB and COMSOL simulations. Figure 29 and Figure 30 show the quadrupole rods, their encasing, and the opening where ions will be injected through.

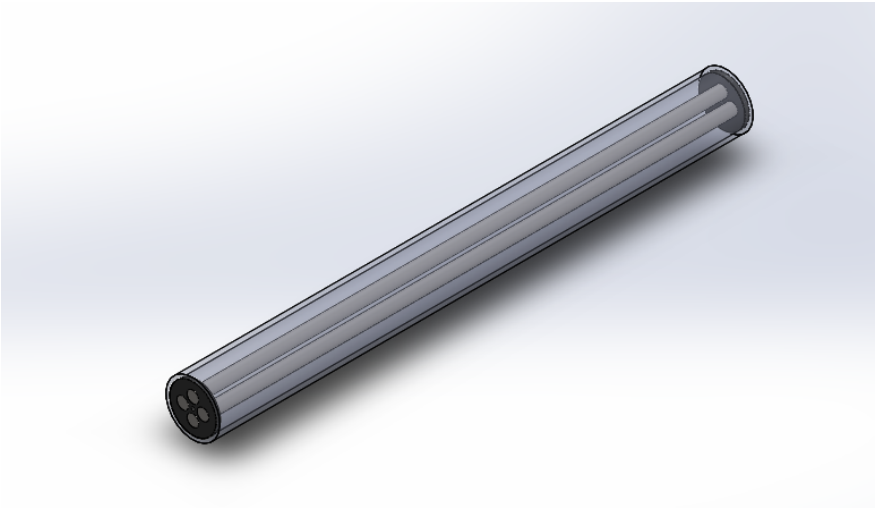

Figure 29. Isometric View of Quadrupole Instrument

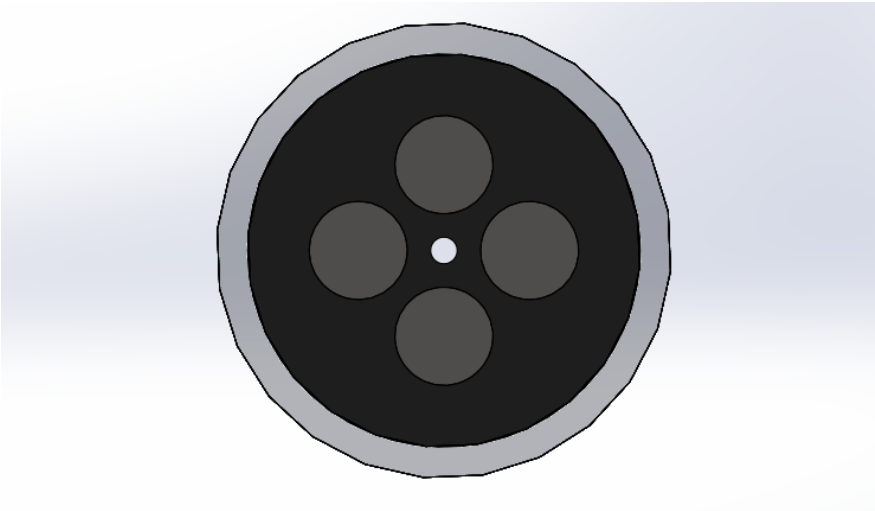

Figure 30. Front Profile of Quadrupole Instrument

A 3U cubesat chassis and motherboard are to be obtained from Pumpkin, Inc. The following are rendering of the chassis and partial assembly that includes the motherboard, the quadrupole instrument, and an ion detector. This is done to aid in visualizing the final arrangement of the system.

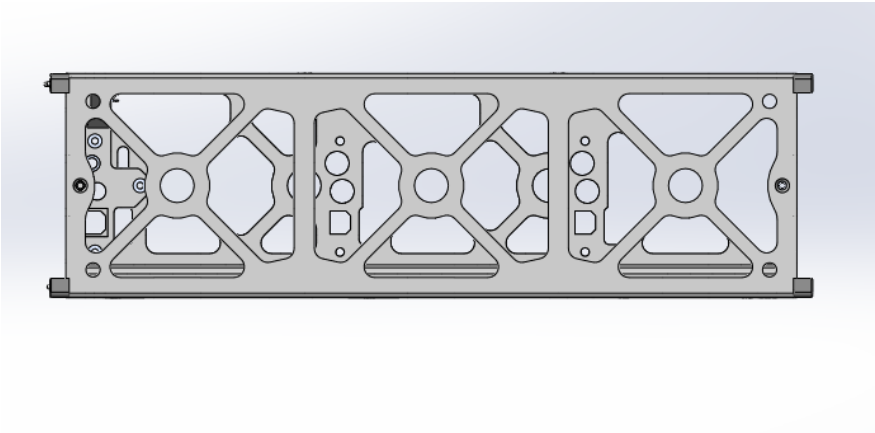

Figure 31. Side Profile of 3U Cubesat Chassis

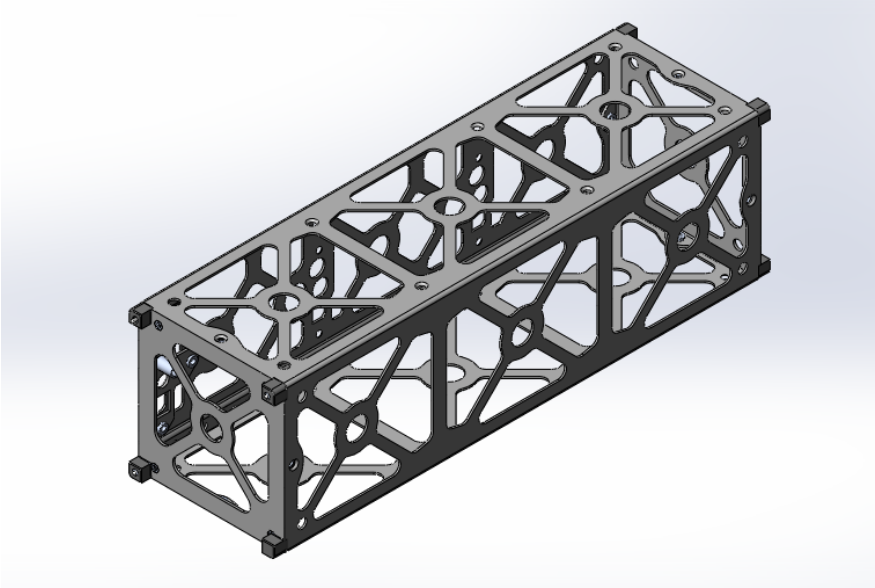

Figure 32. Isometric View of 3U Cubesat Chassis

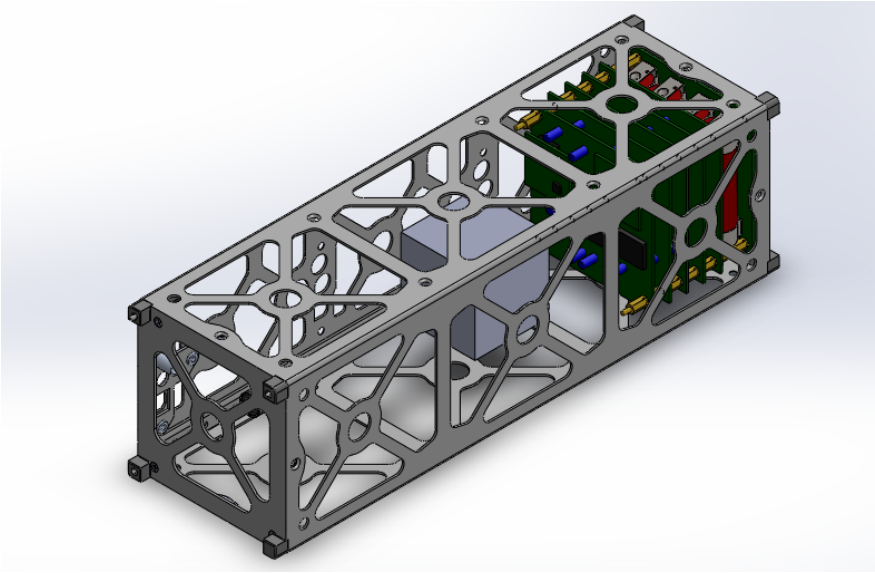

Figure 33. Isometric View of Partial Assembly

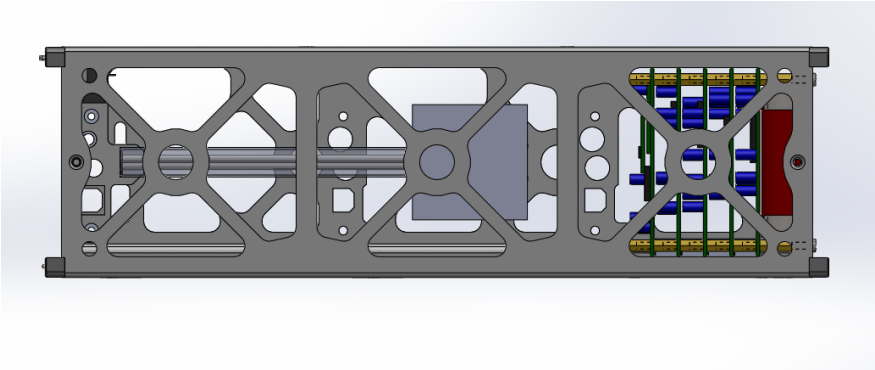

Figure 34. Side Profile of Partial Assembly

VI. Conclusion

The goal of this project was to conduct a preliminary design of a quadrupole mass spectrometer with the capacity of being integrated into a 3U cubesat chassis. This instrument was designed with the purpose of characterizing the abundance of oxygen within Europa's atmosphere. Through carefully tuning the a and q Mathieu coefficients, it was demonstrated that the instrument could be sized to fit within the payload of a 3U cubesat. Voltage requirements for the D.C. and the R.F. potentials were calculated and demonstrated to favor O^{2-} ions. Further work will need to be focused on the feasibility of such a system; most importantly, the power requirements, radiation protection from Jupiter's magnetosphere, and the advantages over current technologies.

Appendix

Matlab Code for Mathieu Stability Diagram

```
Copyright (c) 2012, Siva Srinivas Kolukula
All rights reserved.

Redistribution and use in source and binary forms, with or without
modification, are permitted provided that the following conditions
   are
met:

* Redistributions of source code must retain the above copyright
notice, this list of conditions and the following disclaimer.
* Redistributions in binary form must reproduce the above copyright
notice, this list of conditions and the following disclaimer in
the documentation and/or other materials provided with the
   distribution

THIS SOFTWARE IS PROVIDED BY THE COPYRIGHT HOLDERS AND CONTRIBUTORS
   "AS IS"
AND ANY EXPRESS OR IMPLIED WARRANTIES, INCLUDING, BUT NOT LIMITED TO
   , THE
IMPLIED WARRANTIES OF MERCHANTABILITY AND FITNESS FOR A PARTICULAR
   PURPOSE
ARE DISCLAIMED. IN NO EVENT SHALL THE COPYRIGHT OWNER OR
   CONTRIBUTORS BE
LIABLE FOR ANY DIRECT, INDIRECT, INCIDENTAL, SPECIAL, EXEMPLARY, OR
CONSEQUENTIAL DAMAGES (INCLUDING, BUT NOT LIMITED TO, PROCUREMENT OF
SUBSTITUTE GOODS OR SERVICES; LOSS OF USE, DATA, OR PROFITS; OR
   BUSINESS
INTERRUPTION) HOWEVER CAUSED AND ON ANY THEORY OF LIABILITY, WHETHER
    IN
CONTRACT, STRICT LIABILITY, OR TORT (INCLUDING NEGLIGENCE OR
   OTHERWISE)
ARISING IN ANY WAY OUT OF THE USE OF THIS SOFTWARE, EVEN IF ADVISED
   OF THE
POSSIBILITY OF SUCH DAMAGE.

N = 30 ;                    % Order of the Hill's Determinant
T = cell(1,4) ;             % Cell array to store Hill determinant
   matrices
EE = cell(1,4) ;
epsilon = -40:0.01:40 ;
for i = 1:length(epsilon)
        e = epsilon(i) ;
        a = e*ones(N,1) ;       % Sub diagonal elements
        c = e*ones(N,1) ;       % Super diagonal elements
        % Hill determinants for odd sine and cosine coefficients
```

```
        ndeto = 2*N+1 ;
        bo = (1:2:ndeto).^2 ;   % Diagonal elements
        T1 = diag(a,-1)+diag(bo)+diag(c,+1) ;
        T1(1,1) = 1+e ;
        T{1} = T1 ;             % Odd cosine determinant matrix
        T1(1,1) = 1-e ;
        T2 = T1 ;
        T{2} = T2 ;             % Odd sine determinant matrix
        % Hill determinants for even sine and cosine coefficients
        ndete = 2*(N+1) ;
        be = (2:2:ndete).^2 ;   % Diagonal elements
        T3 = diag(a,-1)+diag(be)+diag(c,+1) ;
        T{3} = T3 ;             % Even cosine determinant matrix
        T4 = zeros(size(T3)) ;
        T4(1,1) = 0 ;T4(1,2) = e ;T4(2,1) = 2*e ;
        T4(2:end,2:end)=T3(1:end-1,1:end-1) ;
        T{4} = T4 ;             % Even sine determinant matrix
        % Calculate the Eigenvalues of the Determinant matrices
        for j = 1:4
                E = eig(T{j}) ;
                EE{j}(:,i) = E ;
        end
end
epsilon = epsilon' ;
E1 = EE{1}' ;
E2 = EE{2}' ;
E3 = EE{3}';
E4 = EE{4}' ;
E = [E1 E2 E3 E4] ;
figure ;
plot(epsilon,E,'b')
title('Mathieu Stability Diagram')
xlabel('a') ;
ylabel('q') ;
hold on ;
plot(-epsilon,-E,'b')
g = linspace(0,1);
h=g*0.3;
plot(g,h,'k--')
axis([0,1,-0.3,0.3])
PlotAxisAtOrigin

function PlotAxisAtOrigin
%PlotAxisAtOrigin Plot 2D axes through the origin

% GET TICKS
X=get(gca,'Xtick');
Y=get(gca,'Ytick');
```

```
% GET LABELS
XL=get(gca,'XtickLabel');
YL=get(gca,'YtickLabel');

% GET OFFSETS
Xoff=diff(get(gca,'XLim'))./80;
Yoff=diff(get(gca,'YLim'))./80;

% DRAW AXIS LINEs
plot(get(gca,'XLim'),[0 0],'k');
plot([0 0],get(gca,'YLim'),'k');

% Plot new ticks
for i=1:length(X)
plot([X(i) X(i)],[0 Yoff],'-k');
end;
for i=1:length(Y)
plot([Xoff, 0],[Y(i) Y(i)],'-k');
end;
```

MATLAB Code for Ion Motion

```
%% Aerospace Engineering Master's Project
% Quadrupole Mass Spectrometer - Ion Motion Simulations

%% Oxide Ion Motion
% Parameter Definitions
omega = 2*pi*4E6;                    % angular frequency (Hz)
e = 1.60E-19;                        % electron charge (Coulomb)
a_u = 0.21;                          % Mathieu coefficient
q_u = 0.7;                           % Mathieu coefficient
m = 2.6569E-26;                      % mass of an O2- ion (kg)
r_o = 2.4133E-3;                     % inscribed radius (m)
A = 2                                % Accelerating Voltage (V)
U = (a_u*m*omega^2*r_o^2)/(8*e);     % DC Voltage (V)
V = (q_u*m*omega^2*r_o^2)/(4*e);     % AC Voltage (V)
vz = sqrt((2*e*A)/m)                 % initial ion velocity (m/s)
tim = .127/vz;                       % time for ion to travel a
   distance
% equivalent to the length of the
% instrument

sim('MP_mathieuX')
figure
plot(t,x)
axis([0,tim,-r_o,r_o])
title('O^{2-} Ion Motion Within X-Z Plane')
xlabel('Time (s)')
ylabel('X-Position from Origin (m)')

sim('MP_mathieuY')
figure
plot(t,y)
axis([0,tim,-r_o,r_o])
title('O^{2-} Ion Motion Within Y-Z Plane')
xlabel('Time (s)')
ylabel('Y-Position from Origin (m)')

%% Sulfide Ion Motion
clear a_u q_u vz tim

m = 5.3137E-26;                      % mass of an S2- ion (kg)
vz = sqrt((2*e*A)/m)                 % initial ion velocity (m/s)
tim = .127/vz;                       % time for ion to travel a
   distance
% equivalent to the length of the
% instrument
a_u = (8*e*U)/(m*omega^2*r_o^2);     % Mathieu coefficient
q_u = (4*e*V)/(m*omega^2*r_o^2);     % Mathieu coefficient
```

```
sim('MP_mathieuX')
figure
plot(t,x)
axis([0,tim,-r_o,r_o])
title('S^{2-} Ion Motion Within X-Z Plane')
xlabel('Time (s)')
ylabel('X-Position from Origin (m)')

sim('MP_mathieuY')
figure
plot(t,y)
axis([0,1.5E-6,-r_o,r_o])
title('S^{2-} Ion Motion Within Y-Z Plane')
xlabel('Time (s)')
ylabel('Y-Position from Origin (m)')

%% Nitride Ion Motion
clear a_u q_u vz tim

m = 2.3248E-26;                     % mass of an N3- ion (kg)
vz = sqrt((2*e*A)/m)                % initial ion velocity (m/s)
tim = .127/vz;                      % time for ion to travel a
   distance
% equivalent to the length of the
% instrument
a_u = (8*e*U)/(m*omega^2*r_o^2);    % Mathieu coefficient
q_u = (4*e*V)/(m*omega^2*r_o^2);    % Mathieu coeficient

sim('MP_mathieuX')
figure
plot(t,x)
axis([0,1E-6,-r_o,r_o])
title('N^{3-} Ion Motion Within X-Z Plane')
xlabel('Time (s)')
ylabel('X-Position from Origin (m)')

sim('MP_mathieuY')
figure
plot(t,y)
axis([0,tim,-r_o,r_o])
title('N^{3-} Ion Motion Within Y-Z Plane')
xlabel('Time (s)')
ylabel('Y-Position from Origin (m)')

function x_ddot = fcn(x,e,m,r_o,U,V,Om,c)
%Mathieu equation representing ion trajectory motion within the
   quadrupole
```

```
x_ddot = -(((2*e)/(m*r_o^2))*(U-V*cos(Om*c)))*x;
end

function y_ddot = fcn(y,e,m,r_o,U,V,Om,c)
%Mathieu equation representing ion trajectory motion within the
   quadrupole

y_ddot = (((2*e)/(m*r_o^2))*(U-V*cos(Om*c)))*y;
end
```

Acknowledgments

First and foremost, I would like to thank my wonderful parents, fantastic brother, marvelous sister, and spectacular girlfriend. You all are relentless in providing me with support during any and every occasion. *Gracias, con todo mi corazón. Los quiero más de lo que se imaginan.*

Next, I would like to thank my project advisor, Dr. Olenka Hubickyj from the Physics and Astronomy Department. I greatly appreciate all the words of encouragement, your sound advice, and your endless enthusiasm.

Lastly, and certainly not least, I would like to thank Dr. Nikos Mourtos, Director of the Aerospace Engineering Department. Your unbound patience with all students is admirable. I am thankful to have been a part of the Aerospace Engineering Department under your supervision.

References

[1]Steklov, A.F., "Atmospheres of Planetary Satellites. I-Possibility of Existence," *Astronomicheskii Vestnik*, Vol. 11, 1977, pp. 219-225.

[2]Cassidy, T.A., Johnson, R.E., McGrath, M.A., Wong, M.C., and Cooper, J.F. "The Spatial Morphology of Europa's Near-Surface O2 Atmosphere," *Icarus*, Vol. 191, No. 2, 2007, pp. 755-764.

[3]Hall, D.T., Strobel, D.F., Feldman, P.D., McGrath, M.A., and Weaver, H.A., "Detection of an Oxygen Atmosphere on Jupiter's Moon Europa," *Nature*, Vol. 373, No. 6516, 1995, pp. 677-679.

[4]Orlando, T.M., McCord, T.B., and Grieves, G.A., "The Chemical Nature of Europa's Surface Material and the Relation to a Subsurface Ocean," *Icarus*, Vol. 177, No. 2, 2005, pp. 528-533.

[5]Grayzeck, Ed. "NASA-NSSDC-Experiment-Details," Nssdc.gsfc.nasa.gov., N.p., 2015. Web. 3 Mar. 2015.

[6]Goldbook.iupac.org., "IUPAC Gold Book - Solvation," N.p., 2015. Web. 3 Mar. 2015.

[7]Cooper, J.F., and Khurana, K.K., "Jovian Magnetospheric Environment Science," *Icarus*, Vol. 178, No.2, 2005, pp. 295-296.

[8]Watson, J.T., and Sparkman, O.D., *Introduction to Mass Spectrometry: Instrumentation, Applications, and Strategies for Data Interpretation*, John Wiley and Sons, 2007.

[9]Dawson, P.H., *Quadrupole Mass Spectrometry and its Applications*, 2013.

[10]Cassidy, T.A., Johnson, R.E., and Tucker, O.J., "Trace Constituents of Europa's Atmosphere", *Icarus*, Vol. 201, No.1, 2009, pp. 182-190.

[11]Johnson, R.E., Lanzerotti, L.J., and Brown, W.L., "Planetary Applications of Ion Induced Erosion of Condensed-Gas Frosts," *Nuclear Instruments and Methods in Physics Research*, Vol. 198, No.1, 1982, pp. 147-157.

[12]Chart, S. (2015). File Exchange - MATLAB Central. Mathworks.com. Retrieved 17 September 2015, from $http://www.mathworks.com/matlabcentral/fileexchange/35355-stability-chart/all_files$.